6-2018

Electrostatic Alignment of Electrospun PEO Fibers by the Gap Method Increases Individual Fiber Modulus in Comparison to Non-Aligned Fibers of Similar Diameter

Christopher Fryer

Meghan Scharnagl

Christine C. Helms
University of Richmond, chelms@richmond.edu

Recommended Citation

Fryer, Christopher, Meghan Scharnagl, and Christine Helms. "Electrostatic Alignment of Electrospun PEO Fibers by the Gap Method Increases Individual Fiber Modulus in Comparison to Non-Aligned Fibers of Similar Diameter." *AIP Advances* 8, no. 6 (June 2018): 065023. https://doi.org/10.1063/1.5027812.

Electrostatic alignment of electrospun PEO fibers by the gap method increases individual fiber modulus in comparison to non-aligned fibers of similar diameter

Christopher Fryer, Meghan Scharnagl, and Christine Helms[a]
University of Richmond, Richmond, Virginia 23173, USA

(Received 6 March 2018; accepted 14 June 2018; published online 22 June 2018)

Studies on the alignment, physical and mechanical properties of individual electrospun fibers provide insight to their formation, production and optimization. Here we measure the alignment, diameter and modulus of individual fibers formed using the electrostatic gap method. We find electrostatic alignment produces fibers with a smaller diameter than their nonaligned counterparts have. Therefore, due to the dependence of fiber modulus on diameter aligned fibers have a higher modulus. Furthermore, we show that aligned and nonaligned fibers of the similar diameter have different moduli. Aligned fibers have a modulus 1.5 to 2 times larger than nonaligned fibers of the similar diameter. https://doi.org/10.1063/1.5027812

INTRODUCTION

The process of electrospinning is a valuable methodology for generating nanofibers due to its reliability and simplicity.[1] One can produce fibers of variable diameters easily, with fibrous mats made up of fibers with diameters ranging from tens of nanometers to a few microns. In terms of nanofiber potential, applications range across fields including filtration, photonic materials, electronics, drug delivery, reinforcements in composite developments, and tissue engineering. However, many of these applications require control of fiber diameter, orientation and mechanical properties.[2–6] For example, one can use substrate rigidity and topography to direct cell differentiation and cell migration important to tissue engineering.[7–9] Aligned fibers with controllable diameter and modulus are of specific interest in nerve-tissue engineering as one can produce them to mimic axons and myelinated nerve fibers.[10,11]

One can electrospun many natural and synthetic polymers with promise in a variety of applications. In particular, a large amount of research has focused on optimized spinning parameters for and studied resultant electrospun polyethylene oxide (PEO) fibers and mats.[12–18] PEO is a very simple polymer to electrospun and is dissolved in water. In addition, potential applications of electrospun PEO include soft tissue engineering applications, drug delivery, biosensors, and electronics.[19–26]

When producing electrospun fibers, changes in spinning parameters lead to alterations in fiber properties. For example, researchers have studied the effects of various electrospinning parameters, such as working distance, polymer conductivity, polymer concentration and voltage, on fiber diameter, mechanics and alignment in an effort to aid the development of nanoscale materials.[27–29] Many groups have written papers on the optimization of electrospinning parameters for various polymers and applications.[30–33]

Under a basic electrospinning setup, one uses a single plate collector and the positioning of collected fibers is ultimately determined by the chaotic whipping of the charged fiber jet producing unwoven mats of electrospun fibers. However, due to the desire to control the orientation of the collected fibers various experimental methods exist to produce nanofiber alignment including mechanical alignment,[34–37] near-field alignment,[38,39] and electrostatic alignment.[40–42] Electrostatic

[a]Author to whom correspondences should be addressed: chelms@richmond.edu

alignment utilizes manipulations of the electric field between the needle and collector to influence the orientation of the produced fibers. The addition of electrodes or adjusting the geometry of the grounded collecting plate can produce electric fields that result in fiber alignment.[41,43,44] For example, Li et al. reported a method, which we use in this paper, of introducing a gap into the collecting plate to manipulate the electric field into producing parallel, aligned fibers.[44]

When using mechanical alignment methods, such as a spinning mandrel, studies have reported differences between aligned and nonaligned electrospun fiber mats. For example, Yan et al. found fibers in mechanically aligned mats had a smaller diameter and higher tensile modulus.[45] Kim et al. showed the modulus and strength of mats aligned by rotating mandrel increase with mandrel speed, while the extensibility decreases with increasing mandrel speed.[46] Zussman et al. attributed stretching of the electrospun fiber during collection on a spinning wheel to necking during fiber failure.[47] This mechanical stretching during collection also contributes to changes in fiber modulus as Brennan et al. demonstrated increased modulus and decreased elongation in electrostatically aligned fibers undergoing a mechanical post drawing technique.[48] Studies, like Brennan et al., of individual fibers, are necessary to distinguish between the effects of network morphology and individual fiber alterations to network properties. Many studies on the effect of alignment on electrospun fiber modulus, have examined fiber mats where network morphology and a distribution of fiber diameters plays a large role in mechanical properties. Therefore, studies of individual fibers are necessary to determine the effect of alignment on individual fibers and remove the effects of network morphology and fiber diameter.

Due to the size of individual electrospun fibers, fewer studies have investigated individual fiber properties; however, the body of work on individual electrospun fibers is growing. Works studying fiber diameter and mechanics have shown fiber diameter has a direct impact on individual fiber modulus, toughness and strength.[49–53] This diameter dependence is attributed to the molecular orientation and morphology within the fiber.[18,49,54] Individual fiber studies have also reported toughness, strength and extensibility of individual fibers,[50] as well as, size dependent, stress relaxation.[55] These studies on individual fibers provide insight that one can use to improve the understanding of fiber formation and fiber optimization. In this paper, we investigate electrostatic alignment by parallel plate collectors and its effect on individual fiber properties including modulus and diameter.

MATERIALS AND METHODS

Substrate preparation

As previously reported,[56–58] we used soft lithography by means of a PDMS stamp to produce a striated surface with 14 μm wide ridges and 10 μm wide groves at a depth of 11.5 μm. The surface was formed on top of a 60mm x 24mm, #1.5, microscope cover glass by pressing the PDMS stamp into drop of Norland Optical Adhesive-81 (NOA-81, Norland Products, Cranbury, NJ). NOA-81 was cured for 90 seconds with UV light (365nm) (handheld UV curing lamp, Edmund Optics, USA).

Fiber production

We produced a polymer solution of 8 % PEO by weight in deionize water. The solution was placed in a 5 ml disposable syringe connected by tygon tubing to a 27-gauge blunt tip needle. The syringe was placed in a syringe pump and dispensed at a rate of 1 ml/hr. We produced fibers by applying 18kV (Gamma High Voltage Research Inc, Ormond Beach, FL) to the needle which was place at a distance of 20 cm from the grounded collector and substrate. We collected fibers on their respective substrates for 1 to 5 minutes, therefore the density of fibers on the samples was similar to those shown in Figure 2a and 2b.

For collection of nonaligned fibers, we utilized a continuous aluminum sheet as the grounded collecting plate and collected fibers onto the striated surface by placing it immediately on top of the aluminum. For collection of aligned fibers, defined as being parallel to one another in spatial orientation, we used two parallel aluminum plates as grounded collectors. The gap between the grounded collectors was 8 cm unless otherwise indicated. The striated substrate was placed in the gap between the aluminum plates for collection of aligned fibers (Figure 1a).

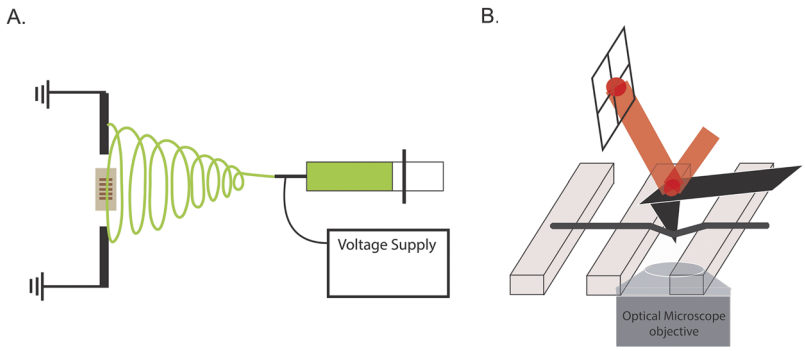

FIG. 1. (a) Aligned fibers were produced using the electrospinning gap method. The needle of a syringe filled with 8 % PEO was connect to 18 kV. Two collectors were grounded and separated by a distance of 8 cm. A striated surface made of UV curing adhesive with features on the order of 10 microns formed by a micromoulding technique, was placed between the grounded collectors for collection of aligned fibers. (b) An AFM was used to manipulate individual fibers and obtained stress-strain curves. The force applied to the fiber is related to the cantilever and laser deflection measured in the photodiode. The AFM is situated atop an optical microscope for visualization of fibers and manipulation.

Fiber alignment

Gap separation was tested at 4cm, 6 cm, 8 cm, and 10 cm to determine the effect of gap separation on fiber alignment. Fibers were collect on glass slides and were imaged using an optical microscope (40x, Axio Observer A1, Zeiss, USA). Image J software (NIH, USA) was used to measure the angle of deviation between the fiber and a normal line drawn perpendicular to the top of the image.

Diameter measurements

Two methods were used to determine fiber diameter. First, a scanning electron microscope (SEM) (6360 LV, JEOL, Peabody, MA) was used to measure the diameter of electrospun fibers. Fibers were sputter coated with palladium (Desk IV, Denton Vacuum, Moorestown, NJ) and imaged at 10,000 X magnification and 16 kV. Image J software was then used to measure fiber diameter.

Second, during fiber modulus measurements, an atomic force microscope (AFM) in intermittent contact mode was used to determine fiber diameters. Diameter measurements were performed immediately prior to fiber manipulations. Scans were performed on the ridges adjacent to the well where the fibers were manipulated with a scan range of 7 by 7 μm with a scan rate of 0.7 Hz. The height retrace was used to determine the diameter of the fibers.

AFM force calibration

Electrospun fiber manipulations were performed using a combined AFM (MFP-3D-Bio, Asylum, USA) and inverted optical microscope (Axio Observer A1, Zeiss, USA). Images and visualization of fiber manipulation were obtained using an AxioCam microscope camera and Zen software (Zeiss, USA). During AFM manipulation, the forces applied to the cantilevers were calculated by treating the cantilever as a torsional spring in accordance with Equation 1.

$$F = \kappa' x L_s \tag{1}$$

As the cantilever stretches an individual fiber, it undergoes torsional rotation, which results in a lateral shift of the cantilever laser in the AFM photodiode. The lateral voltage changes measured by the photodiode are denoted as x in Equation 1. L_s denotes a lateral sensitivity constant to convert the voltage changes into changes in meters. This constant was experimentally determined by measuring the slope of the voltage verse position graph as the cantilever pressed against a glass slide. This process was repeated for each cantilever used to generate unique lateral sensitivity values. The k' denotes the effective spring constant of the cantilever and is determined by Equation 2.

$$\kappa' = \frac{\kappa}{h^2}\frac{L}{L'} \tag{2}$$

The torsion constant κ is found by utilizing the Sader method of determining torsional cantilever spring constants, which incorporates properties of the cantilever as well as its resonant frequency in a fluid.[59] The fluid in this case is air and the thermal frequency was determined in the range of 10 to 100 kHz. The Sader constant is corrected in Equation 2 to more accurately represent our cantilevers where h is the height of the cantilever tip, and $\frac{L}{L'}$ is the length of the cantilever over the distance from the base to the position of the vertical tip.[59]

Modulus data

During fiber collection, nanofibers spun onto the striated surface become attached to the ridges and suspended over the wells. Nanofibers with segments perpendicular to the ridges were selected for manipulation by atomic force microscopy as shown in Figure 1b. As previously reported,[57,58,60] fibers were pulled by the cantilever and the lateral deflection of the cantilever was used to compute the modulus of the fibers.

The cantilever deflection and position were recorded using an Asylum compatible controlled step script written in house (https://facultystaff.richmond.edu/~chelms/publications.html) that allows for exact cantilever positioning and collection of lateral deflection and position data at every step. Cantilever tips with a force constant 0.3 N/m were used (CSC37, Mikromasch, USA).

Cantilevers tips were positioned in the center of the wells containing fiber perpendicular to the ridges and lowered either 3.5 μm to 4 μm in the z-direction with respect to the tops of the adjacent ridges. Data was collected at strain rates ranging from 1 %/s to 6 %/s. The behavior of the fiber during the manipulation was monitored with the optical microscope. Stress-strain curves were plotted to determine the moduli of the manipulated fibers. Initial modulus values for each fiber were determined by calculating the slope of the linear relationship between stress and strain in the regime of 0.001 to 0.01 strain.

Electric field model

A two dimensional electric field model was created in Mathematica (Wolfram Research, Champaign, Il, USA). Laplaces' equation (equation 3), in the area between and surrounding the needle and grounding plates, was numerically solved using the Jacobi relaxation method.

$$\nabla^2 V = 0 \tag{3}$$

Dirichlet boundary conditions at a distance of 4 times the working distance were set to zero and the needle and grounding plates were fixed at 18 kV and zero, respectively. We then calculated the gradient of potential to determine the electric field (equation 4). The electric field in the x-direction, the direction of alignment was then reported when referring to the alignment field.

$$E = -\nabla V \tag{4}$$

Statistical testing

Modulus and diameter measurements were collected for aligned and nonaligned fibers. These mechanical properties were compared across the fiber alignment groups using 2-tailed t-tests assuming equal variances.

RESULTS AND DISCUSSION

Larger collector separation increases fiber alignment

The gap method produced aligned PEO fibers (Figure 2). We measured and compared fiber alignment for collector separations of 4 cm, 6 cm, 8 cm, and 10 cm, using SEM and optical microscopy. To account for any rotation of the sample during fiber collection or imaging, we fit the data to a Gaussian distribution and report the variance from the mean as it represents the width of the distribution of measured angles. As seen in figure 2c, as the gap distance increased the width of the distribution decreased, therefore, the alignment of electrospun PEO fibers increased with increasing space between the collectors (3 samples at each gap distance with roughly 20 fibers from each sample

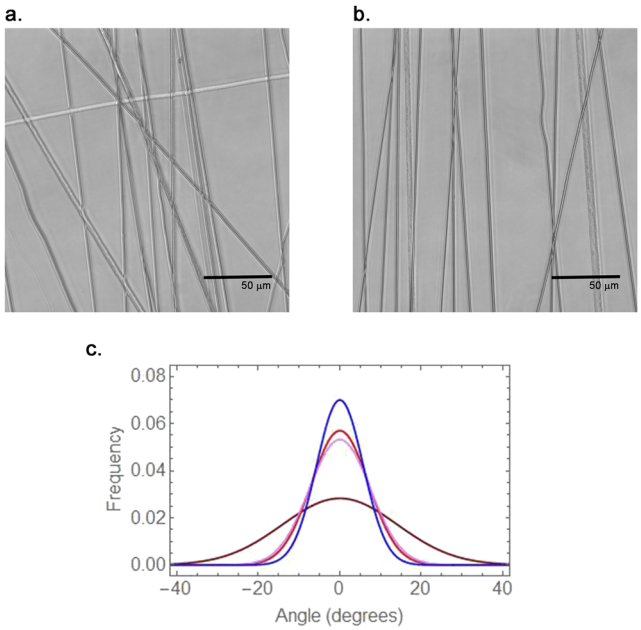

FIG. 2. Optical images of fibers spun on glass slides were used to determine the influence of gap width with ranges from 4 cm (a) to 10 cm (b) on fiber alignment. Fiber angles were measured verses the normal and calculated the variance in each set of data. (c) is a plot of a Gaussian distribution for each gap separation (4 cm – brown, 6 cm – red, 8 cm – pink, 10 cm – blue) based off the measured variance. The 4 cm separation had the highest variance and the 10 cm had the lowest.

were measured). At a gap distance of 4 cm, 6 cm, 8 cm, and 10 cm the data was distributed about the normal with a variance of 200, 49, 57, and 33 respectively. We saw no significant difference in the sample variance, between 6 cm, 8 cm and 10 cm gap distances, although there is a trend of increased fiber alignment with increased collector separation.

To explain this trend in fiber alignment we developed an electric field model to calculate the electrostatic field in the region of fiber formation. A 2D computational model of the electric field using Jacobi Relaxation method showed changing the gap separation alters the strength of the transverse electric field (Figure 3). Increasing the plate separation from 4 cm to 10 cm, increases the electric field in the plane of the collectors 44 %. Our data support that this increase in transverse electric field increases fiber alignment. However it is important to mention, residual charge on the fibers after deposition can lead to electrostatic repulsion between fibers and add complexity to the mechanism of fiber alignment.[43] In addition, the degree of alignment of electrospun fibers decreases with increased fiber density in the region.[61]

Electrostatic alignment produces smaller diameter fibers

We produced electrospun fibers with identical working distance, PEO concentration, voltage, and feed rate (20 cm, 8 % by weight, 18 kV, 1 ml/hr, respectively). In our electrospinning setup, we produced aligned fibers using the gap method with plate separation of 8 cm and nonaligned fibers using a solid collector. SEM measurements of fiber diameters revealed aligned fibers had a smaller average diameter than nonaligned fibers, 215 +/- 4 nm verses 467 +/- 10 nm, respectively.

During alignment, fibers attach first to one collector and then continue to whip before attaching to the opposite collector. This additional whipping and stretching due to the electric field across the gap may be responsible for the decreased diameter measurements of aligned fibers. Interestingly, our results differ from other studies using smaller gaps sizes that reported no difference in diameter between aligned and nonaligned fibers.[62,63] However, the almost 10-fold larger gap separation results in a larger alignment electric field and therefore electrostatic force on the fiber.

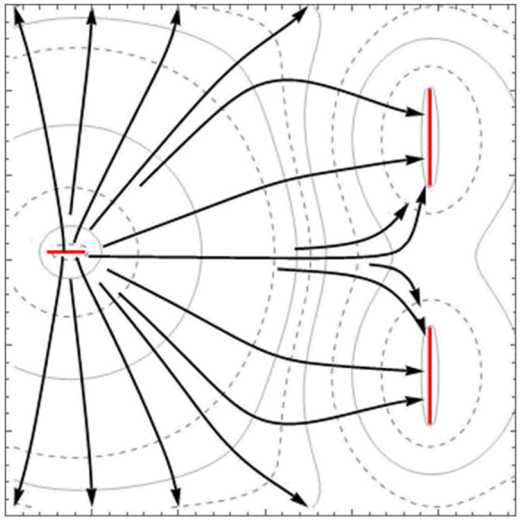

FIG. 3. A plot of the electric field shows the transverse element of the electric field in the region between the collection plates. The red lines indicate the charged needle and the grounded collector plates. Dotted lines represent equipotential lines. Solid black line indicate the direction of the electric field.

Diameter vs modulus

Due to severe strain softening the initial modulus, slope of the stress-strain curve up to 1 % strain, is reported. In agreement with previously published data[49–53,64] we found smaller fibers had a higher modulus than larger fibers (Figure 5). Factors such as crystallinity, molecular arrangement and surface tension can influence the modulus of fibers.

Arinstein et al. and Papkov et al argued a decrease in diameter confined molecular orientation in amorphous regions of electrospun fibers and this molecular confinement was responsible for the increase in fiber modulus of small diameter fibers.[50,54] Lim et al. used AFM to visualize surface morphology as a function of diameter and found a higher degree of molecular orientation in smaller fibers compared to larger fibers.[18] Stachewicz et al demonstrated a shell-core morphology to their electrospun PVA fibers, where the shell showed greater molecular alignment and maintained a constant thickness as fiber diameter changed.[65] Since the shell maintained a constant thickness as the fiber diameter decreased, a higher percentage of the fiber cross section is part of the oriented shell region. As expected, our data support increased orientation and crystallinity due to spatially limited molecular confinement in smaller diameter fibers (Figure 5).

Modulus of aligned vs nonaligned

As shown in figure 4, aligned fibers had smaller diameters than nonaligned fibers. Therefore, due to the modulus dependence on diameter the modulus of aligned fibers was greater than nonaligned fibers produce under the same voltage, concentration, working distance and flow rate.

However, to investigate the effect of electrostatic alignment on modulus, independent of diameter, we used a subset of the aligned and nonaligned fiber populations of similar diameter. Previous studies comparing at aligned and nonaligned fiber moduli tested the properties of the entire mat. Therefore, fiber diameter and network architecture contributions were included in the data. In order to remove the effects of fiber diameter and network architecture we compare individual fiber moduli of electrostatically aligned and nonaligned fibers. Interestingly, we found when we compared the modulus of aligned fibers and nonaligned fibers of similar diameter, aligned fibers continued to have a larger modulus than nonaligned fibers (Figure 6). The average modulus of aligned fibers was approximately 1.5 to 2 times larger than their nonaligned counterparts.

Our data support an increase in fiber modulus due to the electrostatic field produced by the collector configuration. This result is consistent with Kakade et al., who showed electrostatic alignment of fibers lead to increased polymer chain orientation within the fibers[62] and Kimura et al. who measured

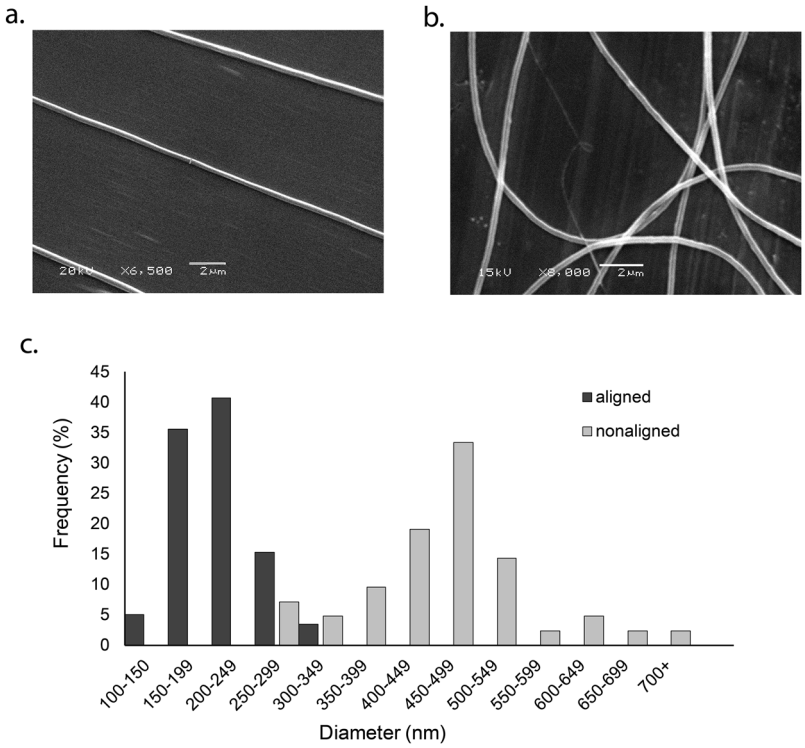

FIG. 4. SEM images of aligned (a) and nonaligned (b) electrospun fibers. (c) Histogram showing the distribution of diameters of aligned (mean: 215 nm ± 41 nm) and nonaligned fibers (mean: 467 nm ± 98 nm). A minimum of 3 samples with approximately 20 fibers per sample were used to determine the diameter. $p < 0.0001$.

molecular orientation by FTIR in fibers aligned using the gap method. Interestingly, these studies reported no change in fiber diameter due to electrostatic alignment. This discrepancy may result from the different gap separations used in the studies and therefore the different alignment electric fields.

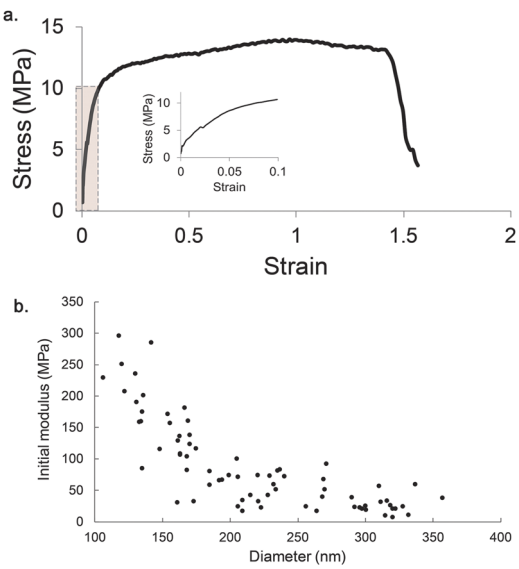

FIG. 5. (a) A typical stress-strain curve for an electrospun PEO fiber. The region emphasized with a gray box is shown in the inset and displays the immediate strain softening of the fibers. (b) The initial modulus of electrospun PEO showed a strong dependence on diameter. Over the recorded range from approximately 125 nm to 350 nm the initial modulus increased by a factor of 10.

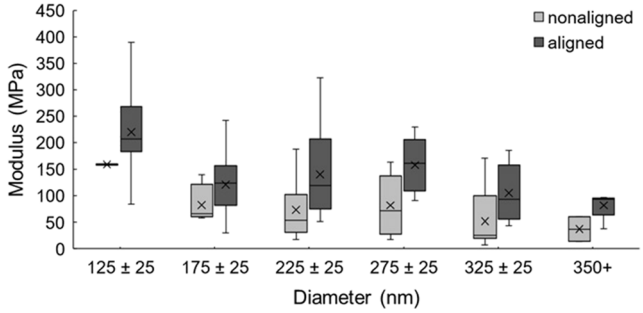

FIG. 6. A box and whiskers plot of the modulus vs diameter data for aligned (dark gray) and nonaligned (light gray). In all diameter ranges the average value of the modulus for aligned fibers is larger than the average modulus for nonaligned (denoted with an x). The plot also indicates the minimum modulus, maximum modulus, median modulus and interquartile values for each diameter range, since there was a large variance in the data.

Although, the gap separations used were much smaller than those employed in this study were, they found increased molecular alignment along the fiber axis when they increased the gap separation.[63]

The change in fiber diameter due to electrostatic alignment has a larger effect on fiber modulus than the effect of fiber alignment independent of diameter. The average diameter of aligned fibers was 215 nm with a corresponding modulus of approximately 50 MPa, while the average diameter of nonaligned fibers was 450 nm with an average modulus of approximately 10 MPa. This is approximately a 5-fold increase due to fiber diameter. When we compared the modulus of fibers with similar diameters, aligned fibers had a 2-fold increase in modulus compared to nonaligned fibers. This data suggest that the increase in molecular orientation due to transverse electrostatic alignment may be small compared to the molecular arrangement due to the longitudinal electric field and spatial confinement.

Recent advances and current work in electrostatic alignment focus on maintaining alignment over longer spinning times, increasing the length of aligned fibers, and decreasing the diameter distribution of aligned mats.[61,66,67] Changes to the electrostatic field are achieved using negatively charged collectors with u-shaped and cylindrical geometries as well as additional negative electrodes introduced along the path of the jet.[61,66,67] Our work specifically shows electrostatic alignment by grounded parallel plates changes to the modulus of electrospun fibers. However, it is reasonable to hypothesize that adjustments to the electrostatic field through other electrostatic methods, independent of changes in individual fiber diameter can effect individual fiber moduli. Therefore, our results justifies further research in to the effect of electrostatic alignment on individual fiber moduli employing these techniques.

CONCLUSIONS

Electrostatic alignment of electrospun fibers using the gap method produces fibers whose alignment increases with increasing transverse electric field strength and increasing gap separation. The strength of electrostatic alignment is sufficient to stretch fibers so the fiber diameter of aligned fibers is less than the diameter of nonaligned fibers. This smaller diameter gives electrostatically aligned fibers a higher modulus than their nonaligned counterparts have. Furthermore, when we compare fibers of similar diameter, electrostatically aligned fibers have an increased modulus when compared to nonaligned fibers. Alignment of electrospun fibers using the gap method, not only increases fiber modulus through a mechanism related to fiber diameter but also through a mechanism distinct from fiber diameter.

ACKNOWLEDGMENTS

This work was supported by the Thomas F. and Kate Miller Jeffress Memorial Trust, Bank of America, N.A., Trustee and the University of Richmond School of Arts and Sciences.

[1] T. C. Mokhena, V. Jacobs, and A. S. Luyt, "A review on electrospun bio-based polymers for water treatment," Express Polymer Letters **9**(10), 839–880 (2015).
[2] N. A. Melosh *et al.*, "Ultrahigh-density nanowire lattices and circuits," Science **300**(5616), 112 (2003).
[3] K. J. Aviss, J. E. Gough, and S. Downes, "Aligned electrospun polymer fibers for skeletal muscle regeneration," European Cell and Materials **19**, 193–204 (2010).
[4] R. Kessick and G. Tepper, "Electrospun polymer composite fiber arrays for the detection and identification of volatile organic compounds," Sensors and Actuators B: Chemical **117**(1), 205–210 (2006).
[5] N. I. Kovtyukhova and T. E. Mallouk, "Nanowires as building blocks for self-assembling logic and memory circuits," Chemistry – A European Journal **8**(19), 4354–4363 (2002).
[6] M. Ma, R. M. Hill, and G. C. Rutledge, "A review of recent results on superhydrophobic materials based on micro- and nanofibers," J. Adhes. Sci. Technol. **22**(15), 1799–1817 (2008).
[7] X. Sun *et al.*, "Asymmetric nanotopography biases cytoskeletal dynamics and promotes unidirectional cell guidance," Proceedings of the National Academy of Sciences **112**(41), 12557–12562 (2015).
[8] J. Wang, J. W. Petefish, A. C. Hillier, and I. C. Schneider, "Epitaxially grown collagen fibrils reveal diversity in contact guidance behavior among cancer cells," Langmuir **31**(1), 307–314 (2015).
[9] H. Mi *et al.*, "Electrospinning of unidirectionally and orthogonally aligned thermoplastic polyurethane nanofibers: Fiber orientation and cell migration," Journal of Biomedical Materials Research. Part A **103**(2), 593–603 (2014).
[10] T. B. Bini, S. Gao, S. Wang, and S. Ramakrishna, "Poly(l-lactide-co-glycolide) biodegradable microfibers and electrospun nanofibers for nerve tissue engineering: An in vitro study," J. Mater. Sci. **41**(19), 6453–6459 (2006).
[11] A. S. Nain *et al.*, "Control of cell behavior by aligned micro/nanofibrous biomaterial scaffolds fabricated by spinneret-based tunable engineered parameters (STEP) technique," Small **4**(8), 1153–1159 (2008).
[12] R. L. Andersson *et al.*, "Micromechanics of ultra-toughened electrospun PMMA/PEO fibres as revealed by in-situ tensile testing in an electron microscope," Scientific Reports **4**, 6335 (2014).
[13] J. Doshi and D. H. Reneker, "Electrospinning process and applications of electrospun fibers," Journal of Electrostatics **35**(2), 151–160 (1995).
[14] J. Raimund, M. M. Bergshoef, C. M. Batlle, H. Schonherr, and V. G. Julius, "Electrospinning of ultra-thin polymer fibers," Macromol. Symp. **127**(1), 141–150 (1998).
[15] R. Jaeger, H. Schonherr, and G. J. Vancso, "Chain packing in electro-spun poly(theylene oxide) visualized by atomic force microscopy," Macromolecules **29**, 7634–7636 (1996).
[16] J. M. Deitzel, J. Kleinmeyer, D. Harris, and N. C. Beck Tan, "The effect of processing variables on the morphology of electrospun nanofibers and textiles," Polymer **42**(1), 261–272 (2001).
[17] B. Jiaxing, L. I. Clarke, and R. E. Gorga, "Effect of constrained annealing on the mechanical properties of electrospun poly(ethylene oxide) webs containing multiwalled carbon nanotubes," J. Polym. Sci. Part B: Polym. Phys. **54**(8), 787–796 (2016).
[18] C. T. Lim, E. P. S. Tan, and S. Y. Ng, "Effects of crystalline morphology on the tensile properties of electrospun polymer nanofibers," Appl. Phys. Lett. **92**(14), 141908 (2008).
[19] P. Basu *et al.*, "PEO–CMC blend nanofibers fabrication by electrospinning for soft tissue engineering applications," Materials Letters **195**, 10–13 (2017).
[20] B. M. Baker *et al.*, "Sacrificial nanofibrous composites provide instruction without impediment and enable functional tissue formation," Proc. Natl. Acad. Sci. U. S. A. **109**(35), 14176–14181 (2012).
[21] J. W. Gatti, M. C. Smithgall, S. M. Paranjape, R. J. Rolfes, and M. Paranjape, "Using electrospun poly(ethylene-oxide) nanofibers for improved retention and efficacy of bacteriolytic antibiotics," Biomed. Microdevices **15**(5), 887–893 (2013).
[22] J. G. Fernandes *et al.*, "PHB-PEO electrospun fiber membranes containing chlorhexidine for drug delivery applications," Polymer Testing **34**, 64–71 (2014).
[23] L. Ma, L. Deng, and J. Chen, "Applications of poly(ethylene oxide) in controlled release tablet systems: A review," Drug Dev. Ind. Pharm. **40**(7), 845–851 (2014).
[24] P. Nagar, I. Chauhan, and M. Yasir, "Insights into polymers: Film formers in mouth dissolving films," Drug Invention Today **3**(12), 280–289 (2011).
[25] A. K. M. M. Alam, J. P. Yapor, M. M. Reynolds, and Y. V. Li, "Study of polydiacetylene-poly (ethylene oxide) electrospun fibers used as biosensors," Materials **9**, 202 (2016).
[26] N. J. Pinto *et al.*, "Electrospun polyaniline/polyethylene oxide nanofiber field-effect transistor," Appl. Phys. Lett. **83**(20), 4244–4246 (2003).
[27] M. Mirjalili and S. Zohoori, "Review for application of electrospinning and electrospun nanofibers technology in textile industry," Journal of Nanostructure in Chemistry **6**(3), 207–213 (2016).
[28] Z. Li and C. Wang (2013) in pp 15–28.
[29] V. Beachley and X. Wen, "Effect of electrospinning parameters on the nanofiber diameter and length," Materials Science & Engineering. C, Materials for Biological Applications **29**(3), 663–668 (2009).
[30] J. Y. Park, I. H. Lee, and G. N. Bea, "Optimization of the electrospinning conditions for preparation of nanofibers from polyvinylacetate (PVAc) in ethanol solvent," Journal of Industrial and Engineering Chemistry **14**(6), 707–713 (2008).
[31] H. M. Khanlou *et al.*, "Prediction and optimization of electrospinning parameters for polymethyl methacrylate nanofiber fabrication using response surface methodology and artificial neural networks," Neural Computing and Applications **25**(3), 767–777 (2014).
[32] S. F. Dehghan *et al.*, "Optimization of electrospinning parameters for polyacrylonitrile-MgO nanofibers applied in air filtration," J. Air Waste Manage. Assoc. **66**(9), 912–921 (2016).
[33] M. K. Leach, Z. Feng, S. J. Tuck, and J. M. Corey, "Electrospinning fundamentals: Optimizing solution and apparatus parameters," Journal of Visualized Experiments: JoVE (47), 2494 (2011).
[34] S. Liu *et al.*, "Assembly of oriented ultrafine polymer fibers by centrifugal electrospinning," Journal of Nanomaterials **2013**.

[35] C. Ayres *et al.*, "Modulation of anisotropy in electrospun tissue-engineering scaffolds: Analysis of fiber alignment by the fast Fourier transform," Biomaterials **27**(32), 5524–5534 (2006).
[36] E. D. Boland, G. E. Wnek, D. G. Simpson, K. J. Pawlowski, and G. L. Bowlin, "Tailoring tissue engineering scaffolds using electrostatic processing techniques: A study of poly(glycolic acid) electrospinning," Journal of Macromolecular Science, Part A **38**(12), 1231–1243 (2001).
[37] A. Theron, E. Zussman, and A. L. yarin, "Electrostatic field-assisted alignment of electrospun nanofibres," Nanotechnology **12**(3), 384–390 (2001).
[38] D. Sun, C. Chang, S. Li, and L. Lin, "Near-field electrospinning," Nano Letters **6**(4), 839–842 (2006).
[39] G. Bisht, S. Nesterenko, L. Kulinsky, and M. Madou, "A computer-controlled near-field electrospinning setup and its graphic user interface for precision patterning of functional nanofibers on 2D and 3D substrates," Journal of Laboratory Automation **17**(4), 302–308 (2012).
[40] L. Liu and A. D. Yuris, "Analysis of the effects of the residual charge and gap size on electrospun nanofiber alignment in a gap method," Nanotechnology **19**(35), 355307 (2008).
[41] M. Pokorny, K. Niedoba, and V. Velebny, "Transversal electrostatic strength of patterned collector affecting alignment of electrospun nanofibers," Appl. Phys. Lett. **96**(19), 193111 (2010).
[42] S. H. Park and D. Yang, "Fabrication of aligned electrospun nanofibers by inclined gap method," J. Appl. Polym. Sci. **120**(3), 1800–1807 (2011).
[43] L. Liu and Y. Dzenis, "Analysis of the effects of the residual charge and gap size on electrospun nanofiber alignment in a gap method," Nanotechnology **19**, 355307 (2008).
[44] D. Li, Y. Wang, and Y. Xia, "Electrospinning of polymeric and ceramic nanofibers as uniaxially aligned arrays," Nano Lett. **3**(8), 1167–1171 (2003).
[45] J. Yan *et al.*, "Effect of fiber alignment in electrospun scaffolds on keratocytes and corneal epithelial cells behavior," Journal of Biomedical Materials Research Part A **100A**(2), 527–535 (2012).
[46] K. W. Kim, K. H. Lee, M. S. Khil, Y. S. Ho, and H. Y. Kim, "The effect of molecular weight and the linear velocity of drum surface on the properties of electrospun poly(ethylene terephthalate) nonwovens," Fibers and Polymers **5**(2), 122–127 (2004).
[47] E. Zussman, D. Rittel, and A. L. Yarin, "Failure modes of electrospun nanofibers," Applied Physics Letters **82**(22), 3958–3960 (2003).
[48] D. A. Brennan *et al.*, "Concurrent collection and post-drawing of individual electrospun polymer nanofibers to enhance macromolecular alignment and mechanical properties," Polymer **103**, 243–250 (2016).
[49] Y. Ji, B. Li, S. Ge, J. C. Sokolov, and M. H. Rafailovich, "Structure and nanomechanical characterization of electrospun PS/clay nanocomposite fibers," Langmuir **22**(3), 1321–1328 (2006).
[50] D. Papkov *et al.*, "Simultaneously strong and tough ultrafine continuous nanofibers," ACS Nano **7**(4), 3324–3331 (2013).
[51] S. Wong, A. Baji, and S. Leng, "Effect of fiber diameter on tensile properties of electrospun poly(ε-caprolactone)," Polymer **49**(21), 4713–4722 (2008).
[52] E. P. S. Tan and C. T. Lim, "Physical properties of a single polymeric nanofiber," Appl. Phys. Lett. **84**(9), 1603–1605 (2004).
[53] C. Pai, M. C. Boyce, and G. C. Rutledge, "Mechanical properties of individual electrospun PA 6(3)T fibers and their variation with fiber diameter," Polymer **52**(10), 2295–2301 (2011).
[54] A. Arinstein, M. Burman, O. Gendelman, and E. Zussman, "Effect of supramolecular structure on polymer nanofibre elasticity," Nature Nanotechnology **2**, 59 (2007).
[55] M. C. Wingert, Z. Jiang, R. Chen, and S. Cai, "Strong size-dependent stress relaxation in electrospun polymer nanofibers," J. Appl. Phys. **121**(1), 015103 (2017).
[56] Y. Xia and G. M. Whitesides, "Soft lithography," Annu. Rev. Mater. Sci. **28**(1), 153–184 (1998).
[57] W. Liu, C. R. Carlisle, E. A. Sparks, and M. Guthold, "The mechanical properties of single fibrin fibers," Journal of Thrombosis and Haemostasis **8**(5), 1030–1036 (2010).
[58] C. R. Carlisle *et al.*, "The mechanical properties of individual, electrospun fibrinogen fibers," Biomaterials **30**(6), 1205–1213 (2009).
[59] C. P. Green *et al.*, "Normal and torsional spring constants of atomic force microscope cantilevers," Rev. Sci. Instrum. **75**(6), 1988–1996 (2004).
[60] C. R. Carlisle, C. Coulais, and M. Guthold, "The mechanical stress–strain properties of single electrospun collagen type I nanofibers," Acta Biomaterialia **6**(8), 2997–3003 (2010).
[61] J. Zhao, H. Liu, and L. Xu, "Preparation and formation mechanism of highly aligned electrospun nanofibers using a modified parallel electrode method," Materials & Design **90**, 1–6 (2016).
[62] M. V. Kakade *et al.*, "Electric field induced orientation of polymer chains in macroscopically aligned electrospun polymer nanofibers," J. Am. Chem. Soc. **129**(10), 2777–2782 (2007).
[63] N. Kimura, H. Kim, B. Kim, K. Lee, and I. Kim, "Molecular orientation and crystalline structure of aligned electrospun nylon-6 nanofibers: Effect of gap size," Macromolecular Materials and Engineering **295**(12), 1090–1096 (2010).
[64] A. Baji, Y. Mai, S. Wong, M. Abtahi, and P. Chen, "Electrospinning of polymer nanofibers: Effects on oriented morphology, structures and tensile properties," Composites Science and Technology **70**(5), 703–718 (2010).
[65] U. Stachewicz, R. J. Bailey, W. Wang, and A. H. Barber, "Size dependent mechanical properties of electrospun polymer fibers from a composite structure," Polymer **53**(22), 5132–5137 (2012).
[66] X. Cai *et al.*, "Electrospinning of very long and highly aligned fibers," J. Mater. Sci. **52**(24), 14004–14010 (2017).
[67] T. Lei *et al.*, "Alignment of electrospun fibers using the whipping instability," Materials Letters **193**, 248–250 (2017).